# 5′-Amino Pyrene Provides a Sensitive, Nonperturbing Fluorescent Probe of RNA Secondary and Tertiary Structure Formation

**Ryszard Kierzek,† Yi Li,‡ Douglas H. Turner,*,‡ and Philip C. Bevilacqua‡**

*Contribution from the Institute of Bioorganic Chemistry, Polish Academy of Sciences, 60-704 Poznan, Noskowskiego 12/14, Poland, and Department of Chemistry, University of Rochester, Rochester, New York 14627*

*Received September 2, 1992*

**Abstract:** Blocked phosphoramidites of 5′-amino-5′-deoxycytidine and 5′-amino-5′-deoxyuridine have been prepared and coupled to the 5′-end of oligoribonucleotides. These 5′-amino RNA oligomers may be readily conjugated to a variety of commercially available amine reactive fluorescent dyes, including succinimidyl ester derivatives. The synthesis, purification, and properties of 5′-pyrene-labeled RNA oligomers are described. These oligomers are shown to be unusually attractive probes for studies of oligomer–oligomer and oligomer–ribozyme interactions. In particular, 5′-pyrene oligomers are stable and very sensitive to environment while having minimal perturbations on the thermodynamics of secondary and tertiary structure formation in RNA. Thus the 5′-positioning of pyrene with a short linker appears to provide an ideal probe for the binding and dynamics of RNA substrates.

## Introduction

The discovery that RNA can catalyze reactions has led to renewed interest in the conformational, binding, and dynamic properties of these macromolecules, since an understanding of these properties will provide a basis for understanding the catalytic strategies of RNA.[1-4] For proteins, fluorescence has provided a powerful tool for studying structure and dynamics.[5-11] Tryptophan and tyrosine provide convenient natural fluorophores, and artificial fluorophores can often be coupled to particular amino acids in a large protein.[12,13] The standard nucleotides in RNA, however, are not sufficiently fluorescent for such applications.[14,15] Thus considerable effort has been applied to developing modified nucleotides with favorable fluorescence properties[14-19] and to coupling artificial fluorophores to nucleotides.[20-24] Modification of proteins with pyrene has provided large fluorescence enhancements.[13,25] For example, modification of actin with pyrene led to a 25-fold fluorescence intensity increase upon polymerization of actin.[13] We report that pyrene coupled with a short linker to the 5′-end of an oligoribonucleotide has unusually favorable characteristics for studies of binding and dynamics involving RNA. In particular, studies of binding to short complementary oligomers and to a group I ribozyme show that the fluorescence intensity differs by more than a factor of 20 depending on the environment but that the pyrene has little effect on complex stability or conformation. Moreover, the fluorescence intensity permits binding and kinetic studies at nanomolar concentrations.

## Experimental Section

**General Materials and Methods.** Succinimido 1-pyrenebutyrate; 5-(and 6-)carboxytetramethylrhodamine succinimido ester; and 5-(and 6-)carboxytetramethylfluorescein succinimido ester were obtained from Molecular Probes, Inc. (Eugene, OR). Lithium azide was prepared according to Hofman-Bang[26] and dried *in vacuo*. Triphenylphosphine, carbon tetrabromide, 9-fluorenylmethyl chloroformate (Fmoc-Cl), and chloro-(diisopropylamino)(β-cyanoethoxy)phosphine were obtained from Aldrich and used without further purification. Diisopropylethylamine and dichloroacetic acid were obtained from Aldrich and distilled before use. 4,4′-Dimethoxytrityl chloride (Dmtr-Cl) was obtained from Chemgenes, Inc. (Waltham, MA). Silica gel 60 H was obtained from E. M. Science and used for column chromatography. Triethylamine was obtained from Fluka. Dimethylformamide (DMF), pyridine, and toluene were obtained from Baker and stored over molecular sieves (4 Å). Dichloromethane was obtained from Fisher and dispensed from a still after refluxing for at least 16 h with 40-mesh $CaH_2$.

Thin-layer chromatography (TLC) was performed with several systems. Silica gel 250F glass plates (Baker) were used with the following eluents:

* To whom correspondence should be addressed.
† Polish Academy of Sciences.
‡ University of Rochester.

(1) Cech, T. R.; Bass, B. L. *Annu. Rev. Biochem.* **1986**, *55*, 599–629.
(2) Guerrier-Takada, C.; Gardiner, K.; Marsh, T.; Pace, N.; Altman, S. *Cell* **1983**, *35*, 849–857.
(3) Cech, T. R.; Herschlag, D.; Piccirilli, J. A.; Pyle, A. M. *J. Biol. Chem.* **1992**, *267*, 17479–17482.
(4) Sugimoto, N.; Tomka, M.; Kierzek, R.; Bevilacqua, P. C.; Turner, D. H. *Nucleic Acids Res.* **1989**, *17*, 355–371.
(5) Lakowicz, J. R. *Principles of Fluorescence Spectroscopy*; Plenum Press: New York, 1983; Chapter 11.
(6) Petrich, J. W.; Longworth, J. W.; Fleming, G. R. *Biochemistry* **1987**, *26*, 2711–2722.
(7) Elöve, G. W.; Chaffotte, A. F.; Roder, H.; Goldberg, M. E. *Biochemistry* **1992**, *31*, 6876–6883.
(8) Munro, I.; Pecht, I.; Stryer, L. *Proc. Natl. Acad. Sci. U.S.A.* **1979**, *76*, 56–60.
(9) Lakowicz, J. R.; Weber, G. *Biochemistry* **1973**, *12*, 4171–4179.
(10) Effink; M. R.; Ghiron, C. A. *Biochemistry* **1977**, *16*, 5546–5551.
(11) Beecham, J. M.; Brand, L. *Annu. Rev. Biochem.* **1985**, *54*, 43–71.
(12) Steinhauser, K. G.; Woolley, P.; Epe, B.; Dijk, J. *Eur. J. Biochem.* **1982**, *127*, 587–595.
(13) Kouyama, T.; Mihashi, K. *Eur. J. Biochem.* **1981**, *114*, 33–38.
(14) Cantor, C. R.; Tao, T. In *Procedures in Nucleic Acid Research;* Cantoni, G. L., Davies, D. R., Eds.; Harper & Row: New York, 1971; Vol. 2, pp 31–93.
(15) Leonard, N. J.; Tolman, G. L. *Ann. N. Y. Acad. Sci.* **1975**, *255*, 43–58.
(16) Leonard, N. J. *CRC Crit. Rev. Biochem.* **1984**, *15*, 125–199.
(17) Tesler, J.; Cruickshank, K. A.; Morrison, L. E.; Netzel, T. L. *J. Am. Chem. Soc.* **1989**, *111*, 6966–6976.
(18) Gildea, B.; McLaughlin, L. W. *Nucleic Acids Res.* **1989**, *17*, 2261–2281.
(19) Ward, D. C.; Reich, E.; Stryer, L. *J. Biol. Chem.* **1969**, *244*, 1228–1237.
(20) Smith, L. M.; Fung, S.; Hunkapiller, M. W.; Hunkapiller, T. J.; Hood, L. E. *Nucleic Acids Res.* **1985**, *7*, 2399–2412.
(21) Draper, D. E. *Nucleic Acids Res.* **1984**, *12*, 989-1002.
(22) Hodges, R. R.; Conway, N. E.; McLaughlin, L. W. *Biochemistry* **1989**, *28*, 261–267.
(23) Ansorge, W.; Sproat, B.; Stegemann, J.; Schwager, C.; Zenke, M. *Nucleic Acids Res.* **1987**, *15*, 4593–4602.
(24) Schubert, F.; Ahlert, K.; Cech, D.; Rosenthal, A. *Nucleic Acids Res.* **1990**, *18*, 3427.
(25) Weltman, J. K.; Szaro, R. P.; Frackelton, R., Jr.; Dowben, R. M.; Bunting, J. R.; Cathou, R. E. *J. Biol. Chem.* **1973**, *248*, 3173–3177.
(26) Hofman-Bang, N. *Acta Chem. Scand.* **1957**, *11*, 581–582.

0002-7863/93/1515-4985$04.00/0 

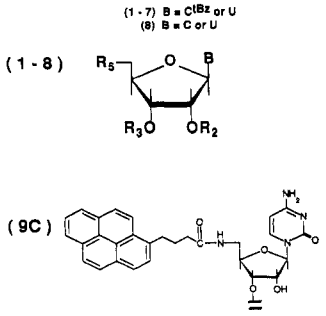


| Derivative | $R_5$ | $R_3$ | $R_2$ |
|---|---|---|---|
| 1 | OH | H | Thp |
| 2 | $N_3$ | H | Thp |
| 3 | $N_3$ | Dmtr | Thp |
| 4 | $NH_2$ | Dmtr | Thp |
| 5 | FmocNH | Dmtr | Thp |
| 6 | FmocNH | H | Thp |
| 7 | FmocNH | P[O(CH2)2CN, N(CH(CH3)2)] | Thp |
| 8 | $NH_2$ | oligomer | H |
| 9 | pyrNH | oligomer | H |

**Figure 1.** Identity of nucleosides at each step in synthesis of 5′-pyrene oligomers. $R_2$, $R_3$, and $R_5$ represent the functional groups attached to the 2′-O, 3′-O, and 5′-C positions, respectively. Derivatives **1-8** are represented in the upper structure; derivative **9C** is represented in the lower structure.

chloroform/methanol 98:2 (v/v) (system A); chloroform/methanol 95:5 (v/v) (system B); chloroform/methanol 9:1 (v/v) (system C); acetone/hexanes/triethylamine 45:45:10 (v/v/v) (system D). In system D, the TLC was soaked with solvent D and dried prior to loading the plate to prevent cleavage of the amidite. Silica gel 500F glass plates (Baker) were used with 2-propanol/$NH_4OH$/water 7:1:2 (v/v/v) (system E). Reverse-phase TLC RP-8 F254 plates (E. M. Science) were used with acetone/water 7:3 (v/v) (system F).

$^1H$ NMR spectra were acquired on General Electric QE-300 and Varian VXR-500S spectrometers and referenced to an internal standard of TMS. $^{31}P$ NMR spectra were acquired on a Bruker AMX-400 spectrometer, referenced to external 1% phosphoric acid, and locked in reference to $CD_3CN$ (MSD isotopes). Ultraviolet (UV) spectra were recorded on a Perkin-Elmer 330 spectrophotometer in methanol for nucleosides and in 50 mM Hepes/25 mM $Na^+$ (pH 7.5) for oligomers. Extinction coefficients were determined on a Gilford 250 spectrophotometer at 70 °C to disrupt any structure. Fluorescence spectra were recorded on a Perkin-Elmer MPF-44A spectrofluorimeter. Infrared (IR) spectra were recorded on a 6020 Galaxy Series FT-IR. Optical melting and stopped-flow experiments were performed as previously described.[27,28] Circular dichroism (CD) spectra were obtained on a Jasco J-40 spectropolarimeter. Conversion to $\Delta\epsilon$ was as previously described.[29] Elemental analyses were performed by Galbraith Laboratories, Knoxville, TN. Low-resolution fast atom bombardment (FAB) mass spectra were performed in a glycerol/1% trifluoroacetic acid matrix by the Midwest Center for Mass Spectrometry.

**Synthetic Procedures.** All compounds in the synthesis are illustrated in Figure 1. Cytidine and uridine derivatives are referred to as the derivative number followed by C or U, respectively. For example, in Figure 1, (**4C$^{tBz}$**) is derivative **4** with B = 4-*N*-(*tert*-butylbenzoyl)cytidine. Gram quantities are specified for synthesis of cytidine derivatives, but mmol ratios are identical for uridine derivatives. Except for (**8**) and (**9**), cytidine derivatives are protected at the 4-N-position with *tert*-butylbenzoyl; uridine derivatives are not N-protected. As appropriate, the presence of Dmtr was probed by exposing the TLC plate to HCl vapors and examining for an orange spot, and the presence of a primary aliphatic amine was examined by a ninhydrin test.[30]

**Synthesis of 4-*N*-(*tert*-Butylbenzoyl-2′-*O*-(tetrahydropyranyl)-5′-azido-5′-deoxycytidine (2C$^{tBz}$).** The starting material, 4-*N*-(*tert*-butylbenzoyl)-2′-*O*-tetrahydropyranylcytidine (**1C$^{tBz}$**), was synthesized as previously described.[31] MS (FAB) *m/z* calcd 488.2 ($MH^+$); obsd 488.3 ($MH^+$, 0.7), 272.1 ($C^{tBz}$ + 2H, 68), 161.1 (tBz, 100). Cytidine derivative **1C$^{tBz}$** (7.58 g, 15.6 mmol) and lithium azide (3.80 g, 77.7 mmol) were coevaporated with anhydrous DMF (3 × 20 mL) to remove any traces of water and dissolved in 78 mL of anhydrous DMF. Triphenylphosphine (4.48 g, 17.1 mmol) was added followed by carbon tetrabromide (5.67 g, 17.1 mmol). After 16 h at room temperature, TLC analysis (system A) indicated completion of reaction. The mixture was evaporated and the residue worked-up with a saturated aqueous solution of sodium bicarbonate and extracted with chloroform (3 × 100 mL). Organic layers were combined, dried with sodium sulfate, and evaporated. FTIR ($CHCl_3$): 2106 $cm^{-1}$($N_3$). $R_f$ (**1C$^{tBz}$**) (system A) 0.11, 0.19; (system B) 0.38, 0.50; (system F) 0.46, 0.50. $R_f$ (**2C$^{tBz}$**) (system A) 0.26, 0.35; (system B) 0.62, 0.88; (system F) 0.30, 0.34. MS (FAB) *m/z* calcd 513.2 ($MH^+$); obsd 513.2 ($MH^+$, 19), 279.1 (100), 272.1 ($C^{tBz}$ + 2H, 53), 161.1 (tBz, 69).

**Synthesis of 2′-*O*-(Tetrahydropyranyl)-5′-azido-5′-deoxyuridine (2U).** **2U** was prepared in a manner identical to that for **2C$^{tBz}$** except the starting material was 2′-*O*-tetrahydropyranyluridine (**1U**)[31] and reaction was complete after 1 h. FTIR ($CHCl_3$): 2106 $cm^{-1}$($N_3$). $R_f$ (**1U**) (system C) 0.47, 0.59; (system F) 0.74, 0.80. $R_f$ (**2U**) (system C) 0.68, 0.73; (system F) 0.55, 0.63.

**4-*N*-(*tert*-Butylbenzoyl)-2′-*O*-(tetrahydropyranyl)-3′-*O*-(dimethoxytrityl)-5′-azido-5′-deoxycytidine (3C$^{tBz}$).** The residue from the previous reaction was evaporated with anhydrous pyridine (3 × 30 mL) and dissolved in anhydrous pyridine (50 mL). Dimethoxytrityl chloride (6.29 g, 18.6 mmol) was added and the reaction left for 40 h at 50 °C. TLC analysis (system A) followed by the HCl test for Dmtr demonstrated completion of reaction. The mixture was worked-up with a saturated aqueous solution of sodium bicarbonate and extracted with chloroform (3 × 75 mL). Organic layers were combined, dried with sodium sulfate, and evaporated. Traces of pyridine were removed by coevaporation with toluene (3 × 20 mL). The mixture was purified by silica gel column chromatography using dichloromethane. Yield for two last reactions: 11.16 g (90.8%). $R_f$ (system A) 0.45; (system B) 0.96; (system F) 0.07. MS (FAB) *m/z* calcd 815.4 ($MH^+$); obsd 815.4 ($MH^+$, 2.0), 303.1 ($Dmtr^+$, 100), 272.1 ($C^{tBz}$ + 2H, 26), 161.1 (tBz, 68).

**2′-*O*-(Tetrahydropyranyl)-3′-*O*-(dimethoxytrityl)-5′-azido-5′-deoxyuridine (3U).** **3U** was prepared in a manner identical to that for **3C$^{tBz}$**. Reactions were very clean for uridine, so that silica gel chromatography was not required at this stage of the synthesis. $R_f$ (system C) 0.84; (system F) 0.16.

**4-*N*-*tert*-(Butylbenzoyl)-2′-*O*-(tetrahydropyranyl)-3′-*O*-(dimethoxytrityl)-5′-amino-5′-deoxycytidine (4C$^{tBz}$).** To **3C$^{tBz}$** (10.44 g, 13.2 mmol), dissolved in methanol (50 mL) and triethylamine (12 mL), was added triphenylphosphine (4.15 g, 15.9 mmol). The mixture was stirred for 1.5 h at room temperature and periodically vented to allow $N_2$ to escape. TLC analysis (system A) followed by the HCl test for Dmtr and the ninhydrin test[30] for the presence of a primary amine indicated completion of reaction. The mixture was evaporated and coevaporated with anhydrous pyridine (3 × 50 mL). $R_f$ (system A) 0.0–0.2; (system B) 0.0–0.2; (system F) 0.0–0.3.

**2′-*O*-(Tetrahydropyranyl)-3′-*O*-(dimethoxytrityl)-5′-amino-5′-deoxyuridine (4U).** **4U** was prepared in a manner identical to that for **4C$^{tBz}$** except reaction took 3 h to complete. $R_f$ (system C) 0.0–0.2; (system F) 0.0–0.3.

TLC plates for **4C$^{tBz}$** and **4U** had a series of spots ($R_f$ = 0.0–0.3) which tested positive for both Dmtr and amine. These spots converted to a single spot upon protection of the amine with 9-fluorenylmethyl chloroformate.

**4-*N*-(*tert*-Butylbenzoyl)-2′-*O*-(tetrahydropyranyl)-3′-*O*-(dimethoxytrityl)-5′-*N*-((9-fluorenylmethoxy)carbonyl)-5′-amino-5′-deoxycytidine (5C$^{tBz}$).** To the residue from the previous reaction dissolved in anhydrous pyridine (50 mL) was added 9-fluorenylmethyl chloroformate (4.05 g, 15.9 mmol), and the reaction mixture was left for 30 min at room temperature. TLC analysis (system A) followed by the HCl test for Dmtr and a negative ninhydrin test[30] for the protection of the amine indicated completion of reaction. The mixture was worked-up with a saturated aqueous solution of sodium bicarbonate and extracted with chloroform (3 × 100 mL). Organic layers were combined, dried with sodium sulfate, and evaporated. Traces of pyridine were removed by coevaporation with toluene (3 × 20 mL). $R_f$ (system A) 0.48; (system B) 0.95; (system F) 0.06. MS (FAB) *m/z* calcd 1011.5 ($MH^+$); obsd 1011.5 ($MH^+$, 0.03), 303.1 ($Dmtr^+$, 100), 161.1 (tBz, 57).

**2′-*O*-(Tetrahydropyranyl)-3′-*O*-(dimethoxytrityl)-5′-*N*-((9-fluorenylmethoxy)carbonyl)-5′-amino-5′-deoxyuridine (5U).** **5U** was prepared in a manner identical to that for **5C$^{tBz}$** except reaction took 2 h to complete. $R_f$ (system C) 0.88; (system F) 0.06, 0.11.

**4-*N*-(*tert*-Butylbenzoyl)-2′-*O*-(tetrahydropyranyl)-5′-*N*-((9-fluorenylmethoxy)carbonyl)-5′-amino-5′-deoxycytidine (6C$^{tBz}$).** To the residue from the previous reaction was added 1 L of 1% dichloroacetic acid in dichloromethane, and the reaction mixture was left at room temperature. Reaction progress was monitored every 5 min by TLC (system A). After 15 min, detritylation was complete. The mixture was immediately neutralized by and worked-up with a saturated aqueous solution of sodium

(27) Petersheim, M.; Turner, D. H. *Biochemistry* **1983**, *22*, 256–263.
(28) Bevilacqua, P. C.; Kierzek, R.; Johnson, K. A.; Turner, D. H. *Science* **1992**, *258*, 1355–1358.
(29) Cantor, C. R.; Schimmel, P. R. *Biophysical Chemistry Part II: Techniques for the Study of Biological Structure and Function*; W. H. Freeman: San Francisco, CA, 1980; Chapter 8.
(30) Gordon, A. J.; Ford, R. A. *The Chemist's Companion: A Handbook of Practical Data, Techniques, and References*; John Wiley and Sons: New York, 1972; p 378.
(31) Markiewicz, W. T.; Biala, E.; Kierzek, R. *Bull. Pol. Acad. Sci.: Chem.* **1984**, *32*, 433–450.

bicarbonate and extracted with chloroform (3 × 100 mL). Organic layers were combined, dried with sodium sulfate, and evaporated. The mixture was purified by silica gel column chromatography and eluted in a 0–3% gradient of methanol in dichloromethane. The product was precipitated into hexanes. Yield for last four reactions: 4.23 g (45.8%), 42% overall yield. $^1$H NMR (mixture of diastereomers, $CDCl_3$, 300 MHz) $\delta$ (ppm): 7.15–7.95 (13 H, m, Fmoc, Bz, H-6), 5.5–5.7 (2 H, m, H-1', H-5), 4.75 (2 H, m, Fmoc), 4.0–4.55 (7 H, m, Fmoc, Thp H-2, H-2', H-3', H-4', H-5', H-5''), 1.2–2.0 (17 H, m, *tert*-butyl, Thp). UV (methanol): $\lambda_{min}$, 233, 257, 285, 295, $\lambda_{max}$ 255, 264, 289, 300, $\lambda_{sh}$ 226, 275, 310 nm. $R_f$ (system A) 0.29, 0.40; (system B) 0.72, 0.86; (system D) 0.33, 0.46; (system F) 0.22. Anal. Calcd for $C_{40}H_{44}N_4O_8$: C, 67.77; H, 6.26; N, 7.91; O, 18.06. Found: C, 67.37; H, 5.74; N, 6.64; O, 17.97. MS (FAB) $m/z$ calcd 709.3 ($MH^+$); obsd 709.3 ($MH^+$, 2.7), 272.1 ($C^{tBz}$ + 2H, 72), 161.1 (tBz, 100).

**2'-*O*-(Tetrahydropyranyl)-5'-*N*-((9-fluorenylmethoxy)carbonyl)-5'-amino-5'-deoxyuridine (6U).** 6U was prepared in a manner identical to that for **6C$^{tBz}$**. The overall yield for synthesis of 6U was 2.15 g/15-mmol scale (26%). $^1$H NMR (mixture of diastereomers, $CD_3CN$, both 300 and 500 MHz) $\delta$ (ppm): 7.85 (2 H, d, Fmoc), 7.68 (3 H, m, Fmoc, H-6), 7.43 (2 H, t, Fmoc), 7.34 (2 H, t, Fmoc), 5.73, 5.83 (1 H, 2d, H-1'), 5.57, 5.58 (1 H, 2d, H-5), 4.75 (2 H, m, Fmoc), 3.9–4.45 (7 H, m, Fmoc, Thp H-2, H-2', H-3', H-4', H-5', H-5''), 1.2–1.8 (8 H, m, Thp). UV (methanol): $\lambda_{min}$ 232, 285, 295, $\lambda_{max}$ 263, 288, 300, $\lambda_{sh}$ 226, 255, 275 nm. $R_f$ (system C) 0.68, 0.71; (system D) 0.24, 0.27; (system F) 0.32, 0.37. Anal Calcd for $C_{29}H_{31}N_3O_8$: C, 63.38; H, 5.68; N, 7.65; O, 23.29. Found: C, 63.30; H, 5.93; N, 7.39; O, 23.30. MS (FAB) $m/z$ calcd 550.2 ($MH)^+$; obsd 550.2 ($MH^+$, 0.4), 179.1 (100).

**4-*N*-(*tert*-Butylbenzoyl)-2'-*O*-(tetrahydropyranyl)-3'-*O*-[(*N*,*N*-diisopropylamino)(β-cyanoethoxy)phosphinyl]-5'-*N*-((9-fluorenylmethoxy)carbonyl)-5'-amino-5'-deoxycytidine (7C$^{tBz}$).** 6C$^{tBz}$ (1.06 g, 1.5 mmol) was dried *in vacuo* overnight. Anhydrous dichloromethane (12 mL) and diisopropylethylamine (0.39 mL, 2.3 mmol) were added and stirred. To the mixture was added dropwise chloro(diisopropylamino)(β-cyanoethoxy)phosphine (0.35 mL, 1.8 mmol), and the reaction mixture was stirred at room temperature. Silica gel TLC (system D) indicated the reaction was over 90% complete after 1 h. The mixture was worked-up with a saturated aqueous solution of sodium bicarbonate and a saturated aqueous solution of sodium chloride, followed by extraction with chloroform (3 × 50 mL). The solution was dried over sodium sulfate and evaporated. The mixture was purified by silica gel column chromatography. The column was eluted in a 40–55% gradient of ethyl acetate in hexanes containing 1% pyridine. Product-containing fractions were identified by TLC (system D), pooled, coevaporated with toluene (2 × 20 mL), and lyophilized from benzene to yield a white powder. Yield for this reaction: 846 mg (64%). $^{31}$P NMR ($CD_3CN$, 162 MHz) $\delta$ (ppm): 150.6, 150.8, 150.9, 151.1 (mixture of diastereomers). $R_f$ (system D) 0.65.

**2'-*O*-(Tetrahydropyranyl)-3'-*O*-[(*N*,*N*-diisopropylamino)(β-cyanoethoxy)phosphinyl]-5'-*N*-((9-fluorenylmethoxy)carbonyl)-5'-amino-5'-deoxyuridine (7U).** 7U was prepared in a manner identical to that for **7C$^{tBz}$**. Unlike the above, 6U was initially insoluble in dichloromethane/diisopropylethylamine; however, upon addition of chloro(diisopropylamino)(β-cyanoethoxy)phosphine, it was readily soluble, as similarly observed with 5'-*N*-(((9-fluorenylmethyl)oxy)carbonyl)-5'-amino-5'-deoxy-2'-deoxythymidine.[20] Yield for this reaction: 648 mg/1.5-mmol scale (60%). $^{31}$P NMR ($CD_3CN$, 162 MHz) $\delta$ (ppm): 150.6, 150.9, 151.3 (mixture of diastereomers). $R_f$ (system D) 0.50.

**Preparation and Purification of Unlabeled Oligoribonucleotides (8).** Oligoribonucleotides were synthesized on solid support following a phosphoramidite approach.[32] Protected 5'-amino phosphoramidite couplings appeared equally efficient as unmodified protected phosphoramidite couplings, as judged by the intensity of failure sequences upon TLC purification. Oligoribonucleotides were subsequently deblocked, purified by TLC, and used directly in the fluorophore coupling reaction without G-10 desalting.[33] Presence of the primary aliphatic amine was confirmed with a ninhydrin test.[30] After purification, 5-μmol-scale syntheses of pentamers $NH_2$CCUCU and $NH_2$UCUCU yielded 44 and 41 $A_{260}$ units (≈2 mg), respectively.

**Preparation and Purification of Labeled Oligoribonucleotides (9).** In a silanized microfuge tube[34] were mixed 20 $A_{260}$ units of purified 5'-amino oligoribonucleotide in 200 μL of autoclaved water, 300 μL of DMF, 50 μL of 1 M sodium carbonate buffer (pH 9.0) (filtered through a 0.2-μm Nalge filter), and 50 μL of the N-hydroxysuccinimidyl ester of carboxyfluorescein, carboxytetramethylrhodamine, or butyrylpyrene (10 mg of dye/100 μL of DMF). The reaction was warmed with a heat gun to dissolve all reactants and left for 16 h at 37 °C. Analytical TLC analysis (system E) indicated completion of reaction. The mixture was concentrated to 250 μL *in vacuo* and purified on silica gel TLC. System C with a silica gel 500F plate was used initially to move excess dye to the top of the plate while leaving the product at the origin (≈2 h). The plate was dried and system E was used on the same plate to move the product (≈5 h). Dye-labeled product was visualized by UV illumination, scraped from the TLC, eluted with water (2 mL) and 50% acetonitrile/water (2 × 2 mL), and concentrated *in vacuo*. Representative TLC's are as follows: $NH_2$CCUCU $R_f$ (system E) 0.08; pyrCCUCU $R_f$ (system E) 0.21. Yield based on $A_{260}$ units for pyrCCUCU and pyrUCUCU: 56 and 63%.

Dye-labeled oligoribonucleotides were further purified by HPLC on a Beckman C-8 column with aqueous buffer of 2 mM sodium phosphate (pH 7.0) (Buffer A) and organic buffer of 2 mM sodium phosphate (pH 7.0) in 75% methanol (Buffer B). A flow rate of 1 mL/min and a gradient of 2% Buffer B/min beginning with 100% Buffer A were used. Yield ($A_{260}$ units) for both pyrCCUCU and pyrUCUCU for the HPLC purification step was 66%. Overall yield for the two-step purification of pyrene-labeled pentamers was ≈40%. To avoid sticking of labeled oligomers, all experiments were performed using silanized tips and tubes.[34]

**Determination of Base Content of Oligomers.** Oligomers (1 $A_{260}$ units/mL) were completely digested by incubation with RNase $T_2$ (0.08 units/μL) in 10 mM Tris, pH 8.0, 1 mM EDTA at 37 °C for 16 h (10-μL total volume). The reaction mixture and Ap, Cp, Gp, and Up markers were then kinased in 70 mM Tris-HCl, pH 7.6, 10 mM $MgCl_2$, 5 mM dithiothreitol, γ-$^{32}$ATP (0.05 μCi/μL), and T4 Kinase (1.0 units/μL). The kinased mixture and markers were run on PEI plates that were presoaked in distilled water for 10 min with occasional shaking and then in methanol for 10 min with occasional shaking and hung to dry. PEI plates were run in 1 M formate buffer, pH 3.5, and bands were visualized by autoradiography, excised, and quantified by scintillation counting in 5 mL of Ecoscint A. CUCU, pyrCUCU, pyrCCUCU, pyrUCUCU, pyrCGUCG, and pyrCUCUCU gave the expected bases in the expected ratios.

**Determination of Extinction Coefficients.** The absorption spectrum of free pyrene overlaps that of RNA. Thus, extinction coefficients for pyrene-labeled oligomers were determined indirectly by two methods. In the first, absorbance, $A$, of pyrCUCU and pyrCCUCU was measured at 260 and 344.5 nm, $\lambda_{max}$, in 50 mM Hepes (pH 7.5) at 70 °C, where the strand is unfolded. Since only pyrene absorbs at 344.5 nm, the ratio of absorbance at 344.5–260 nm for identical solutions gives the following two equations:

$$\frac{A_{344.5}^{\text{pyrCUCU}}}{A_{260}^{\text{pyrCUCU}}} = \frac{\epsilon_{344.5}^{\text{pyrC}}}{\epsilon_{260}^{\text{pyrC}} + \epsilon_{260}^{\text{CUCU}}} \quad (1)$$

$$\frac{A_{344.5}^{\text{pyrCCUCU}}}{A_{260}^{\text{pyrCCUCU}}} = \frac{\epsilon_{344.5}^{\text{pyrC}}}{\epsilon_{260}^{\text{pyrC}} + \epsilon_{260}^{\text{CCUCU}}} \quad (2)$$

Since $\epsilon_{260}$ can be reliably calculated for RNA oligomers,[35] one may solve for $\epsilon_{260}^{\text{pyrC}}$ and $\epsilon_{344.5}^{\text{pyrC}}$. The second method involving disruption of secondary structure by dilution into dimethyl sulfoxide (DMSO) has been described.[36]

## Results

Previous studies of oligomers modified with pyrene on linkers attached to C-5 of thymidine,[37] to 2'-O,[38] or to a central phosphate[39] showed that these modifications affect duplex

(32) Kierzek, R.; Caruthers, M. H.; Longfellow, C. E.; Swinton, D.; Turner, D. H.; Freier, S. M. *Biochemistry* **1986**, *25*, 7840–7846.

(33) He, L.; Kierzek, R.; SantaLucia, J., Jr.; Walter, A. E.; Turner, D. H. *Biochemistry* **1991**, *30*, 11124–11132.

(34) Sambrook, J.; Fritsch, E. F.; Maniatis, T. *Molecular Cloning: A Laboratory Manual Part 3*; Cold Spring Harbor Press: Plainview, NY, 1989; E.1–E.2.

(35) Borer, P. N. In *Handbook of Biochemistry and Molecular Biology: Nucleic Acids*; 3rd ed.; Fasman, G. D., Ed.; CRC Press: Cleveland, OH, 1975; Vol. I, p 597.

(36) Koenig, P.; Reines, S. A.; Cantor, C. R. *Biopolymers* **1977**, *16*, 2231–2242.

(37) Tesler, J.; Cruickshank, K. A.; Morrison, L. E.; Netzel, T. L.; Chan, C.-K. *J. Am. Chem. Soc.* **1989**, *111*, 7226–7232.

(38) Yamana, K.; Gokota, T.; Ozaki, H.; Nakano, H.; Sangen, O.; Shimidzu, T. *Nucleosides and Nucleotides* **1992**, *11*, 383–390.

(39) Yamana, K.; Letsinger, R. L. *Nucleic Acids Symp. Ser.* **1985**, *16*, 169–172.

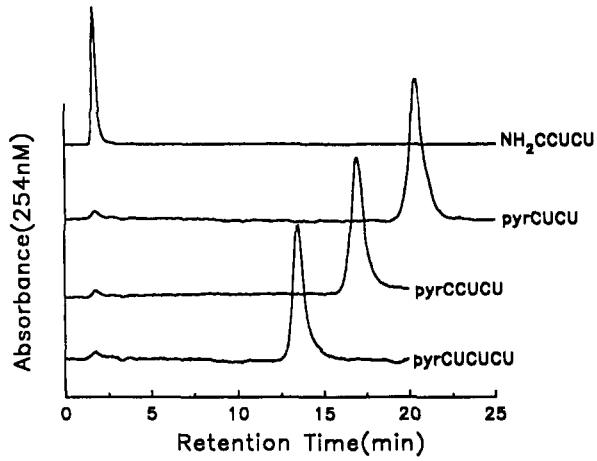


**Figure 2.** Stacked plots of HPLC traces of unmodified pentamer oligomer $NH_2CCUCU$ (derivative **8C**) and 5′-pyrene oligomers pyrCUCU, pyrCCUCU, and pyrCUCUCU (derivative **9C**). Absorbance maxima for each trace are 0.02, using a 1 cm path length cell. HPLC was done on a C-8 column with an aqueous buffer of 2 mM sodium phosphate (pH 7.0) (buffer A) and organic buffer of 2 mM sodium phosphate (pH 7.0)/75% methanol (buffer B). A flow rate of 1 mL/min and a gradient of 2% buffer B/min beginning with buffer A were used.

stability. Addition of an unpaired nucleotide (dangling end) to the 5′-end of an RNA duplex, however, is known to make the free energy change for duplex formation at 37 °C more favorable by only 0.2 kcal/mol on average.[40] This suggests addition of large groups at the 5′-position may be relatively nonperturbing for duplex formation. Molecular modeling suggests a short linker at the 5′-position provides the best chance for a nonperturbing fluorophore, since a short linker precludes intercalation between base pairs. Adding a dye to the 5′-end of the oligomer has the additional advantage that the 3′-end is unchanged. The 3′-end is where chemistry occurs with ribozymes. Thus, compounds of derivative **9** (Figure 1) were chosen as synthetic targets.

The synthesis followed literature procedures whenever appropriate.[20,31,41-43] Thus the starting materials, $\mathbf{1C^{tBz}}$ and **1U**, were the 2′-*O*-tetrahydropyranyl-blocked nucleosides developed by Markiewicz et al.[31] Azide addition closely followed the one-step procedure of Yamamoto et al.[43] Attempts to directly convert the azide to the amine and to protect the amine with a single equivalent of Fmoc-Cl[20] were unsuccessful, as multiple products occurred upon protection. Temporary protection of the 3′-OH with Dmtr-Cl followed by azide reduction by the method of Gibbs and Orgel[42] and amine protection with Fmoc-Cl gave one major product, however. Moreover, syntheses employing the extra Dmtr-Cl protection and deprotection steps led to approximately 2.5 times higher overall yield than syntheses without 3′-OH protection. Preparation of phosphoramidites was similar to that of Smith et al.[20] Incorporation of the modified nucleotides into oligomers followed the method of Kierzek et al.[32] This method has been shown to give 3′–5′ phosphodiester linkages.[32]

Figure 2 illustrates the purity (>95%) of selected 5′-pyrene oligomers. Note that pyrene modification leads to longer retention of the oligomer by HPLC, although less so as oligomer length increases. Presumably this is due to a larger contribution of the negatively charged oligomer. Since there is such a wide difference between modified and unmodified oligomer retention times, purification of pyrene-labeled oligomers by TLC followed by HPLC assures that any unlabeled oligomer is removed. Furthermore, reaction of CCUCU instead of $NH_2CCUCU$ gave no

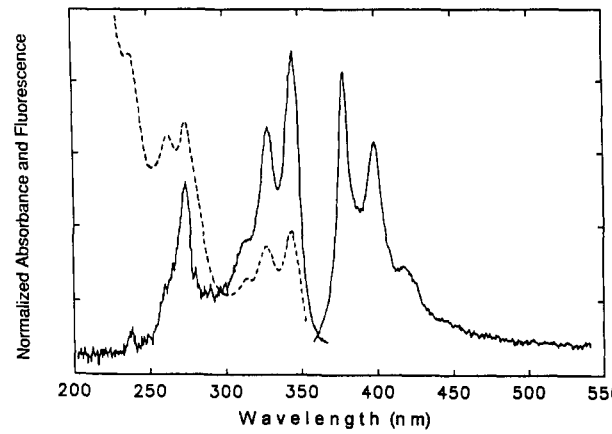


**Figure 3.** Spectral data for pyrCCUCU in 50 mM Hepes/25 mM $Na^+$ (pH 7.5) at room temperature: fluorescence excitation ($\lambda_{max}$ 244, 278.5, 314 (sh), 329, and 343 nm) and emission spectra ($\lambda_{max}$ 377, 397, and 416 nm (sh)) for 2 μM pyrCCUCU (—); absorption spectrum ($\lambda_{max}$ 242, 265, 275, 314, 329, and 344.5 nm) for 3.2 μM pyrCCUCU (- -).

product on TLC, indicating reaction with pyrene is at the 5′-primary aliphatic amine only. Analysis of the base composition of five pyrene-labeled oligomers gave the expected bases in the expected ratios (see Experimental Section). HPLC traces taken after 2 months of storage at −20 °C in water are unchanged, indicating oligomers are chemically stable under these conditions.

The absorption spectrum of single-stranded pyrCCUCU is shown in Figure 3. The $\lambda_{max}$ for absorption of pyrCCUCU and pyrUCUCU is 344.5 nm in 50 mM Hepes (pH 7.5) at 70 °C, while $\lambda_{max}$ for absorption of the reagent succinimido 1-pyrenebutyrate is 341.5 nm in methanol and 342 nm in 4% methanol/96% 50 mM Hepes (pH 7.5) at 70 °C. Red shifts of absorption spectra have been observed for pyrene attached to the 3′-end of poly(U) and poly(C).[36] The extinction coefficient at 344.5 nm, $\epsilon^{pyrC}_{344.5}$, determined by comparison of pyrCCUCU and pyrCUCU (see Experimental Section) is 27 500 $M^{-1}$ $cm^{-1}$. The $\epsilon^{pyrC}_{344.5}$ for pyrCCUCU and pyrCGUCG determined by the DMSO dilution method[36] are 25 200 and 28 300 $M^{-1}$ $cm^{-1}$, respectively. These values are similar to each other and to the values of 32 000 and 37 000 $M^{-1}$ $cm^{-1}$, respectively, for pyreneacetic acid and pyrenebutyric acid attached to the 3′-end of poly(C).[36] The extinction coefficient at 344.5 nm for pyrUCUCU determined by the DMSO dilution method,[36] $\epsilon^{pyrU}_{344.5}$, is 29 000 $M^{-1}$ $cm^{-1}$, similar to the value of 27 300 $M^{-1}$ $cm^{-1}$ for pyrenebutyric acid attached to the 3′-end of poly(U).[36] Optical melts at 280 nm for pyrCCUCU alone and pyrCGUCG alone are noncooperative, indicating these oligomers are single strands for concentrations used here (≤3 μM).

The fluorescence spectrum for pyrCCUCU is shown in Figure 3. The positions and relative intensities of vibronic bands in the fluorescence spectra for all pyrene-labeled oligomers studied are essentially identical, with $\lambda_{max}$ for excitation and emission indicated in Figure 3. The position and relative intensities of the vibronic bands of the fluorescence of pyrene-labeled oligomers are also unchanged upon binding to the group I ribozyme L-21 Sca I[44] and to GGAGGA. GGAGGA mimics the 5′-exon recognition sequence of the ribozyme GGAGGG[45] but is unable to form a pocket with tertiary interactions. (The oligomer GGAGGG is relatively insoluble.[28])

While the shapes of the fluorescence spectra are insensitive to environment, the intensities of fluorescence are extremely sensitive (Figure 4A and B). Upon conjugation to the 5′-amino oligomers, pyrene fluorescence was quenched at least 7-fold (Figure 4A). Pyrene fluorescence is also strongly quenched by acrylamide, 5′-CMP, and 5′-UMP. For example, 25 mM acrylamide quenches

(40) Turner, D. H.; Sugimoto, N.; Freier, S. M. *Ann. Rev. Biophys. Biophys. Chem.* **1988**, *17*, 167–192.
(41) Horwitz, J. P.; Tomson, A. J.; Urbanski, J. A.; Chua, J. *J. Org. Chem.* **1962**, *27*, 3045–3048.
(42) Gibbs, D. E.; Orgel, L. E. *J. Carbohydr., Nucleosides, Nucleotides* **1976**, *3* (*5 and 6*), 315–334.
(43) Yamamoto, I.; Sekine, M.; Hata, T. *J. Chem. Soc., Perkin Trans. 1* **1980**, 306–310.
(44) Zaug, A. J.; Grosshans, C. A.; Cech, T. R. *Biochemistry* **1988**, *27*, 8924–8931.
(45) Waring, R. B.; Scazzocchio, C.; Brown, T. A.; Davies, R. W. *J. Mol. Biol.* **1983**, *167*, 595–605.

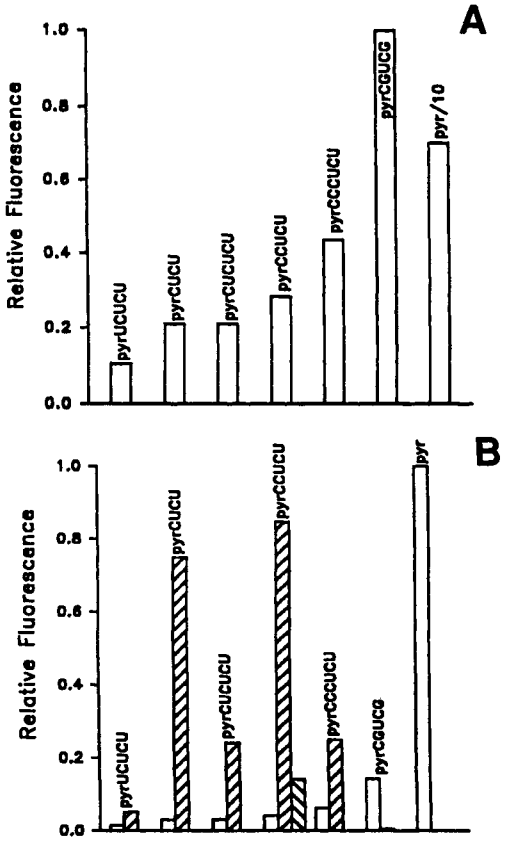


**Figure 4.** Dependence of pyrene fluorescence on environment, excitation at 329 nm and emission at 397 nm. All measurements were taken in 5 mM $MgCl_2$, 135 mM NaCl, and 50 mM Hepes/25 mM $Na^+$ (pH 7.5), at 15 °C. The fluorescence of succinimido 1-pyrenebutyrate is denoted pyr. (A) Relative fluorescence for single-stranded oligomers (□). (B) Relative fluorescence for oligomer complexes with GGAGGA (▨) and L-21 Sca I ribozyme (▨).

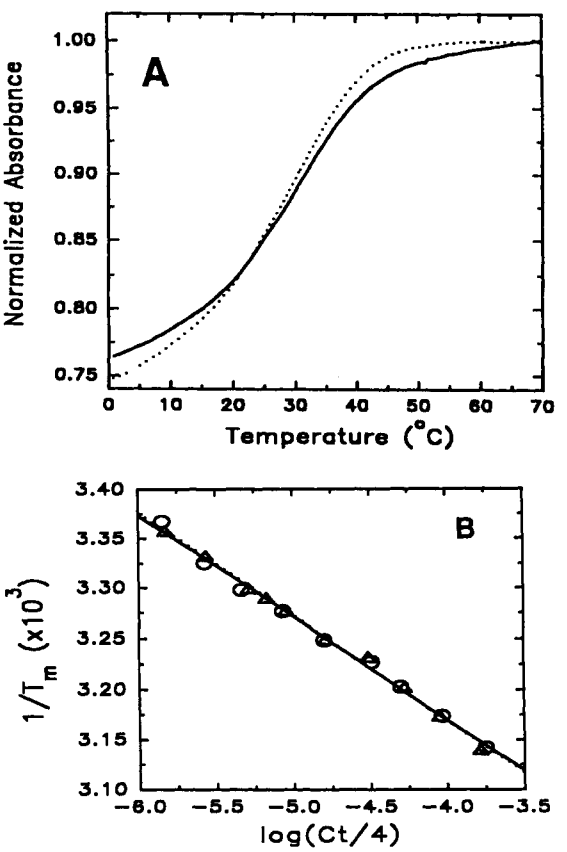


**Figure 5.** (A) Melts of pyrCCUCU/GGAGGA, 20 μM $C_t$, with detection at 280 nm (—) and 344.5 nm (···). For 280 nm, $\Delta G°_{15}$, $\Delta H°$, $\Delta S°$, and $T_m$ are −9.07 kcal/mol, −42.4 kcal/mol, −115.6 eu, and 30.0 °C, respectively; for 344.5 nm, $\Delta G°_{15}$, $\Delta H°$, $\Delta S°$, and $T_m$ are −8.97 kcal/mol, −40.9 kcal/mol, −110.8 eu, and 29.6 °C, respectively. Melts of pyrCCUCU alone are noncooperative at both 280 and 344.5 nm. (B) Reciprocal melting temperature versus the logarithm of $C_t/4$ for duplex formation monitored at 280 nm: (○, —) CCUCU/GGAGGA; (△, ···) pyrCCUCU/GGAGGA. From $1/T_m$ versus log $C_t/4$ plots, $\Delta G°_{15}$, $\Delta H°$, and $\Delta S°$ are −9.11 ± 0.06 kcal/mol, −44.2 ± 1 kcal/mol, and −121.8 ± 3 eu, respectively, for pyrCCUCU/GGAGGA, and −9.17 ± 0.09 kcal/mol, −45.0 ± 1 kcal/mol, and −124.3 ± 4 eu, respectively, for CCUCU/GGAGGA. From the average of fits of melting curves, $\Delta G°_{15}$, $\Delta H°$, and $\Delta S°$ are −9.15 ± 0.2 kcal/mol, −44.1 ± 3 kcal/mol, and −121.2 ± 10 eu, respectively, for pyrCCUCU/GGAGGA, and −9.51 ± 0.3 kcal/mol, −49.7 ± 3 kcal/mol, and −139.6 ± 10 eu, respectively, for CCUCU/GGAGGA.[28]

the fluorescence of succinimido 1-pyrenebutyrate roughly 2-fold. Quenching of pyrene fluorescence has also been observed when pyrene is covalently attached to other nucleic acids.[36-38] The fluorescence of 5'-pyrene single strands varies approximately 10-fold depending upon sequence (Figure 4A). Duplex formation between pyrCCUCU and the oligomer GGAGGA leads to fluorescence enhancement by a factor of approximately 3.5. As illustrated in Figure 4B, binding of 5'-pyrene oligomers to the L-21 Sca I ribozyme leads to an increase in pyrene fluorescence. For example, the fluorescence of pyrCUCU increases 25-fold. Addition of succinimido 1-pyrenebutyrate to the ribozyme under similar conditions led to no change in pyrene fluorescence intensity. The pyrCUCU occupies the binding site that recognizes the 5'-exon for group I splicing[45] whereas pyrCGUCG can occupy the binding site that recognizes the 3'-end of the intron.[46,47] For oligomers binding at the 5'-exon recognition site, the ratio of bound to unbound fluorescence decreases as length increases in the series pyrCUCU, pyrCCUCU, pyrCCCUCU/pyrCUCUCU (Figure 4B). Similar experiments with CCUCU and CUCU labeled at the 5'-end with fluorescein and rhodamine showed less than 10% changes in fluorescence upon binding to ribozyme. Evidently, the emission intensity of pyrene is unusually sensitive to environment.

The effect of pyrene labeling on thermodynamic parameters for duplex formation was studied by optical melting at 280 nm (Figure 5A). For the two-state system A + B ⇌ C,

$$\frac{1}{T_m} = \frac{2.303R}{\Delta H°} \log \frac{C_t}{4} + \frac{\Delta S°}{\Delta H°} \quad (3)$$

Here $T_m$ is the melting temperature in Kelvin and $C_t$ is the total strand concentration. Plots of $1/T_m$ versus log $C_t/4$ for helix formation between GGAGGA and either pyrCCUCU or CCUCU are illustrated in Figure 5B. Thermodynamic parameters are similar with and without the pyrene label.[28] Parameters derived from direct fits of the melts agree within 11% with those derived from plots of $1/T_m$ versus log $C_t/4$, indicating the transitions are consistent with a two-state model (see caption to Figure 5B).[27]

Optical melting of the pyrCCUCU/GGAGGA duplex was also examined at 344.5 nm, $\lambda_{max}$ for absorption by conjugated pyrene. Absorption at 344.5 nm increases cooperatively with temperature, indicating helix formation has a hypochromic effect on pyrene absorption. Fitting of melts of a sample with $C_t$ = 20 μM at either 280 or 344.5 nm give similar results (see caption to Figure 5A).

The effect of pyrene labeling on the conformation of a duplex was studied by circular dichroism (CD). CD spectra for the pyrCCUCU/GGAGGA helix and the CCUCU/GGAGGA helix are illustrated in Figure 6. The spectra are similar and show no ellipticity in the 300–400-nm region, where only pyrene absorbs.

(46) Michel, F.; Hanna, M.; Green, R.; Bartel, D. P.; Szostak, J. W. *Nature* **1989**, *342*, 391–395.
(47) Burke, J. M.; Esherick, J. S.; Burfeind, W. R.; King, J. L. *Nature* **1990**, *344*, 80–81.

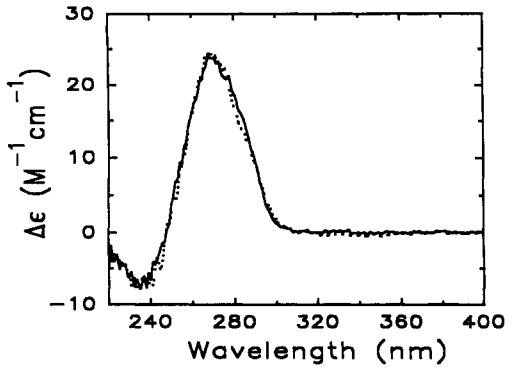


**Figure 6.** Circular dichroism spectra at 15 °C and a $C_t$ concentration of 20 $\mu$M in 5 mM $MgCl_2$, 135 mM NaCl, and 10 mM sodium phosphate/20 mM $Na^+$ (pH 7.5) where essentially all of the strands are in the duplex state: (—) unlabeled CCUCU/GGAGGA; (···) 5′-pyrene-labeled pyrCCUCU/GGAGGA. (50 mM Hepes interfered with the signal at $\lambda <$ 245 nm, although CD's in 5 mM $MgCl_2$, 135 mM NaCl, and 50 mM Hepes/25 mM $Na^+$ (pH 7.5) were similar for unlabeled and pyrene-labeled duplexes between 245 and 400 nm.)

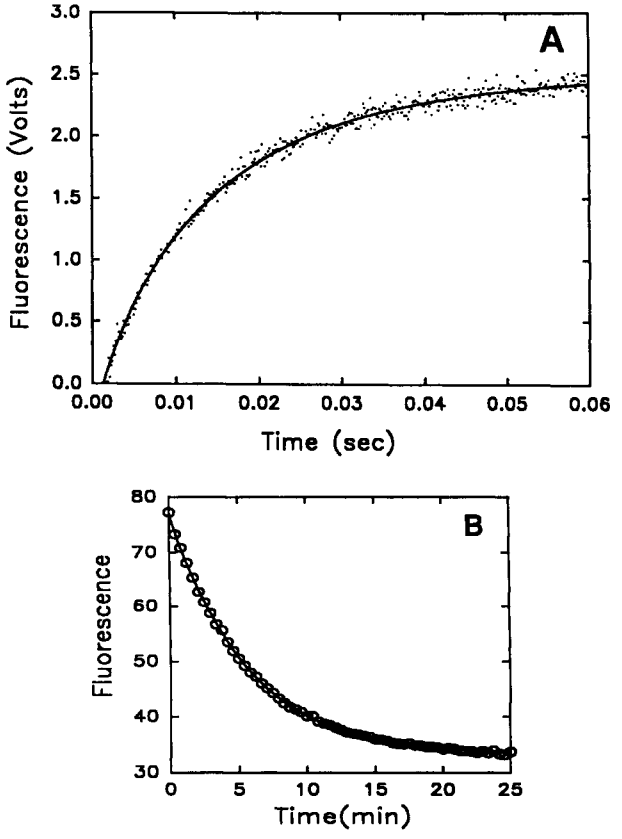


**Figure 7.** Time dependence of pyrCCUCU fluorescence for binding to nucleic acid. All measurements at 15 °C and 5 mM $MgCl_2$, 135 mM NaCl, and 50 mM Hepes/25 mM $Na^+$ (pH 7.5). (A) Rapid-mixing stopped-flow experiment between 1.2 $\mu$M pyrCCUCU and 1.2 $\mu$M GGAGGA (final concentrations). The solid line indicates computer simulation[67,68] of the data to a simple bimolecular mechanism of the type A + B $\rightleftharpoons$ C, with $k_1$ = 52.5 $\mu M^{-1}$ $s^{-1}$ and $k_{-1}$ = 7.3 $s^{-1}$. (B) Chase experiment in which a solution of 40 nM L-21 Sca I, 100 nM pyrCCUCU was mixed with an equivalent volume chase of 10 $\mu$M unlabeled CCUCU. The solid line is a single-exponential fit with a rate of $3.0 \times 10^{-3}$ $s^{-1}$. A chase of 50 $\mu$M unlabeled CCUCU gives a rate of $3.3 \times 10^{-3}$ $s^{-1}$, indicating pyrCCUCU dissociation is rate-limiting.

The 5′-pyrene oligomers are versatile probes of the kinetics of RNA structural changes. Increases (Figure 7A) and decreases (Figure 7B) of pyrene fluorescence can be used to monitor both the rapid (Figure 7A) and slow (Figure 7B) dynamics of RNA secondary (Figure 7A) and tertiary (Figure 7B) structure formation. In Figure 7A, a rapid-mixing experiment in which pyrCCUCU binds to GGAGGA is illustrated. The fluorescence increases upon duplex formation as discussed above. The dynamics for the system follow a simple two-state bimolecular association mechanism. Seven experiments with fluorescence detection centered at 400 nm and the concentration of strands after mixing ranging from 0.2 to 3.2 $\mu$M gave average values of 55 $\mu M^{-1}$ $s^{-1}$ and 6.6 $s^{-1}$ for $k_1$ and $k_{-1}$, respectively.[28] Similar experiments with 280-nm-absorption detection gave rate constants of 58 $\mu M^{-1}$ $s^{-1}$ and 5.7 $s^{-1}$ for $k_1$ and $k_{-1}$, respectively. Thus, pyrene fluorescence accurately reports the same process as base hypochromicity on a rapid millisecond time scale with the advantage of allowing lower oligomer concentrations to be studied (roughly 25 nM duplex).

In Figure 7B, a chase experiment in which pyrene substrate irreversibly dissociates from ribozyme tertiary and secondary contacts is illustrated. In this experiment, 100 nM pyrCCUCU is initially bound to 40 nM L-21 Sca I ribozyme. Upon addition of 10 $\mu$M unlabeled CCUCU, the pyrCCUCU is free to dissociate but effectively cannot reassociate due to the large excess of CCUCU. Thus, the fluorescence decreases with time. Because 25 min is required to follow roughly six half-lives of this dissociation, manual mixing was performed. The curve is single exponential, as expected for a first-order process. Both the single-exponential character of the curve and control experiments in the absence of ribozyme indicate relatively no photobleaching of the pyrene occurred over the 25-min period. Thus, pyrene fluorescence can also be used to monitor slow processes.

Possible structures for the pyrCCUCU/GGAGGA duplex were modeled by energy minimization followed by molecular dynamics for 50 ps followed by another energy minimization using Insight II (version 2.10) and Discover (version 2.80) software from Biosym Technologies with the AMBER force field.[48] Three simulations were performed beginning with an A-form duplex and pyrene stacked either on the 5′-end of the duplex, resting in the major groove, or between these two positions. Hydrogen-bonding lengths within base pairs were constrained between 1.5 and 2.5 Å, and the 3′-dangling A was constrained to help maintain an A-form duplex, as suggested by CD experiments. Initial energy minimization steps led to little movement of pyrene from its initial position, presumably because the structure became trapped in a local energy minimum. Upon dynamics runs, however, all three initial structures led to a similar final structure in which pyrene moved face-to-base-pair-edge in the major groove (Figure 8). The second energy minimization step led to little movement of the structure except that the pyrene ring system, bent during molecular dynamics, became planar again. The lack of interaction between pyrene and the duplex in this structure is consistent with the observation that pyrene does not strongly affect the CD or thermodynamics of the duplex. It is still possible, however, that pyrene stacks on the 5′-end of its own strand, since this interaction is expected to have little effect on the structure and thermodynamics of an RNA duplex. For example, studies of the effects of adding single unpaired nucleotides to the 5′-ends of RNA duplexes indicate they increase duplex stability by only 0.2 kcal/mol on average.[40] This has been attributed to the fact that in standard A-form RNA geometry, a 5′-unpaired nucleotide is distant from the opposite strand.[49]

## Discussion

The goal of this work was to prepare fluorescently labeled oligomers with fluorescence that is sensitive to environment but with binding properties as close as possible to unmodified oligomers. While several phosphoramidite linkers and fluorophores are commercially available for 5′-end labeling, they typically have linkers of nine or more atoms between the 5′-attachment site and the fluorophore. This provides much

(48) Weiner, S. J.; Kollman, P. A.; Nguyen, D. T.; Case, D. A. *J. Comput. Chem.* **1986**, *7*, 230–252.
(49) Freier, S. M.; Alkema, D.; Sinclair, A.; Neilson, T.; Turner, D. H. *Biochemistry* **1985**, *24*, 4533–4539.

**Figure 8.** Computer-generated stereoview of A-form pyrCCUCU/GGAGGA helix with pyrene resting face-to-edge in the major groove. This structure occurred after 50 ps of molecular dynamics, but all structures after 15 ps were similar. The structure has been energy minimized following the dynamics run. Starting structure before dynamics was with pyrene located in a neutral position between the 5'-stacked position and the major groove. Similarly equilibrated structures were found after 50 ps of dynamics when the starting structure had pyrene stacking on the 5'-end of the duplex or resting in the major groove. Pyrene is located in the upper right portion of the figure, and the 3'-A of GGAGGA is located at the bottom of the figure. 2'-OH atoms critical to formation of tertiary structure are enlarged.[53,54]

conformational flexibility that allows the fluorophore to perturb binding interactions. To reduce the conformational flexibility, a phosphoramidite with a 5'-$NH_2$ replacing the 5'-OH was developed. In combination with commercially available succinimido 1-pyrenebutyrate, this provides 5'-end labeling with a 4-atom linker between the 5'-attachment site and the fluorophore. In principle, the linker can be even shorter.

This work presents the first synthesis of blocked 5'-amino ribonucleosides and their incorporation into RNA oligomers. The synthesis largely followed literature procedures available for DNA and RNA monomers.[20,31,41-43] It was, however, necessary to temporarily protect the 3'-OH with Dmtr-Cl before azide reduction and Fmoc-Cl protection. This step was not necessary in the synthesis of 5'-*N*-(((9-fluorenylmethyl)oxy)carbonyl)-5'-amino-5'-deoxy-2'-deoxynucleosides.[20] Perhaps the ribose 2'-O activates the 3'-OH for reaction with Fmoc-Cl.

Ideally, a probe of RNA binding and structure should not affect these properties at either the secondary or tertiary structure level. Effects at the level of secondary structure were studied by comparing the duplexes formed by pyrCCUCU/GGAGGA and CCUCU/GGAGGA. UV melting of these duplexes indicates pyrene has no apparent effect on the thermodynamics of duplex formation (Figure 5B).[28] This contrasts with previous studies where modification with pyrene was found to affect duplex stability. For example, pyrene attached to C-5 of a centrally located thymidine through a six-atom linker increased duplex stability;[37] pyrene attached to a 2'-O through a one-carbon linker increased duplex stability when located on a 5'-terminal ribose and decreased duplex stability when located on an internal ribose;[38] pyrene attached to a centrally located phosphate through a four-carbon linker increased duplex stability.[39] It has been suggested that pyrene intercalates into the duplex in these cases.[37-39] A neutral effect of pyrene on pyrCCUCU/GGAGGA duplex stability suggests pyrene is not intercalating here.

Circular dichroism spectra suggest a 5'-pyrene also does not distort helix geometry. The CD of unmodified and 5'-pyrene duplexes are essentially identical and are similar to spectra for A-form RNA helixes (Figure 6).[50] Moreover, no ellipticity is observed in the region where only pyrene absorbs (300–400 nm), suggesting pyrene is not strongly interacting with the helix and/or is not in a chiral environment. This contrasts with previous studies for pyrene attached to the 3'-ribose of polymeric RNA where duplex formation induced strong ellipticity in the 300–400-nm region.[36] This CD was attributed to direct interaction of pyrene with duplex.

There is also evidence that 5'-pyrene substrates have little or no effect on binding and structure when the labeled oligomer is bound to a ribozyme. In ribozyme-catalyzed transesterification reactions with UCGA, 5'-pyrene-labeled substrates react with the same $k_{cat}/K_m$ for UCGA as do unmodified substrates.[28] These reactions depend on a specific, complex folding of the ribozyme that includes docking of substrate.[51,52] Moreover, 5'-pyrene substrates maintain essentially all of the binding free energy contributions of unmodified substrates for both secondary and tertiary structure formation with ribozyme.[28,53] These observations indicate 5'-pyrene-labeled substrates bind into the catalytic core of the ribozyme without significant perturbation of the binding due to base-pair and minor groove 2'-OH recognition elements and also do not affect the $k_{cat}/K_m$ for ribozyme-catalyzed chemical reactions.

Computer[48] and manual modeling of an A-form pyrCCUCU/GGAGGA helix suggests structural reasons for the observations that pyrene does not perturb binding and structure. Manual model building indicates the three-carbon tether employed in this study is not long enough to allow pyrene to intercalate between base pairs or rest in the minor groove. In addition, known tertiary contacts in this complex involve hydrogen bonds to two 2'-OH's in the minor groove of the recognition helix.[53-56] Lack of perturbation in ribozyme binding and reactivity[28] indicates these 2'-OH tertiary contacts are maintained for pyrene-labeled substrates, consistent with the modeling result that the three-carbon tether is too short to allow pyrene to interact with the minor groove.

Further modeling of the pyrCCUCU/GGAGGA helix indicates the three-carbon tether is long enough to allow pyrene to stack on the 5'-end of the CCUCU strand or on the 3'-A of the GGAGGA strand or to dock in the major groove without distorting A-form geometry. The molecular dynamics study suggests docking in the major groove may be preferred. This is consistent with the CD data and with the observation of identical thermodynamics for duplexes with and without pyrene. Both results suggest pyrene is not interacting strongly with the opposite strand. Compensating effects in which pyrene stabilizes one part of the duplex and equally destabilizes another part cannot be ruled out but are unlikely, as the helix maintains A-form CD identical to that of the unmodified duplex (Figure 6).

Movement of pyrene from a polar to a nonpolar solvent alters the relative vibronic band intensities of pyrene fluorescence.[57,58]

(50) Tunis-Schneider, M. J. B.; Maestre, M. F. *J. Mol. Biol.* **1970**, *52*, 521–541.
(51) Kim, S.-H.; Cech, T. R. *Proc. Natl. Acad. Sci. U.S.A.* **1987**, *84*, 8788–8792.
(52) Michel, F.; Westhof, E. *J. Mol. Biol.* **1990**, *216*, 585–610.
(53) Bevilacqua, P. C.; Turner, D. H. *Biochemistry* **1991**, *30*, 10632–10640.
(54) Pyle, A. M.; Cech, T. R. *Nature* **1991**, *350*, 628–631.
(55) Saenger, W. *Principles of Nucleic Acid Structure*; Springer Verlag: New York, 1984; Chapter 10.
(56) Pyle, A. M.; Murphy, F. L.; Cech, T. R. *Nature* **1992**, *358*, 123–128.
(57) Nakajima, A. *Bull. Chem. Soc. Jpn.* **1971**, *44*, 3272–3277.
(58) Kalyanasundaram, K.; Thomas, J. K. *J. Am. Chem. Soc.* **1977**, *99*, 2039–2044.

These changes have been primarily attributed to changes in pyrene–solvent dipole–dipole interactions.[57,58] Additionally, studies of pyrene monomer interacting with micelles[58] and of polymerization of pyrene-modified actin[13] showed changes in the relative vibronic band intensities. The absence of perturbations in the relative vibronic band intensities upon pyrCCUCU binding to GGAGGA or L-21 Sca I suggests pyrene is still in a polar environment, also consistent with the prediction from molecular dynamics.

Ideally, the fluorescence of a probe for RNA structure should be strongly dependent on environment. This is observed for 5′-pyrene. For example, even with single-stranded oligomers the fluorescence intensity of pyrCGUCG is approximately 10-fold that of pyrUCUCU, but still 7-fold less than that of free succinimido 1-pyrenebutyrate. Since pyrene fluorescence is strongly quenched by acrylamide, 5′-CMP, and 5′-UMP, quenching of fluorescence upon conjugation to oligomer may be due to quenching by the amide bond in the tether, by the bases in the oligomer, or by both. The dependence of fluorescence on sequence for single strands is not a simple nearest-neighbor or even next-nearest-neighbor effect. For the series pyrCUCU/pyrCUCUCU, pyrCCUCU, and pyrCCCUCU, the fluorescence increases as the number of consecutive cytidines at the 5′-terminus increases. pyrUCUCU has less fluorescence than any of the pyrC oligomers. Thus, quenching of pyrene fluorescence appears to have a complex sequence dependence.

The fluorescence enhancement upon duplex formation between pyrCCUCU and GGAGGA is 3.5-fold. Evidently, a helical environment for a 5′-pyrene yields greater fluorescence. In comparison, formation of duplexes results in decreased fluorescence for pyrene attached to the 3′-end of the strand via a modified ribose[36] or for pyrene centrally positioned via a thymidine linker.[37] Formation of duplexes with 2′-*O*-pyrene conjugate RNA oligomers leads to 15-fold increases in fluorescence if the modified ribose is at the 5′-end. The thermodynamics of these duplexes are affected by the pyrene, however, whereas those for pyrene coupled through the 5′-amino are not.

The fluorescence of pyrCCUCU increases 21-fold upon binding to the L-21 Sca I ribozyme (Figure 4B). This is a 6-fold larger increase than observed for binding to the oligomer GGAGGA, which forms the same base pairs as the ribozyme binding site. This indicates the binding site on the ribozyme is considerably different from a single-stranded GGAGGA oligomer. The fluorescence increase of pyrUCUCU is only 3.5-fold compared to 21-fold for pyrCCUCU, making the final pyrUCUCU ribozyme complex 16-fold less fluorescent than the pyrCCUCU complex. Thus, pyrene fluorescence in the catalytic core also depends at least on the identity of the pyrene nearest neighbor. There may be a number of different factors influencing the fluorescence of pyrene oligomers. Whatever these factors, however, 5′-pyrene oligomer fluorescence is clearly sensitive to the nucleic acid sequence, to secondary structure formation, and to tertiary structure formation. Moreover, the changes observed are unusually large. For example, binding of εACUCU to a circular form of the same ribozyme resulted in only a 50% decrease in fluorescence.[59]

Mixing experiments indicate 5′-pyrene oligomers are useful for probing both rapid and slow RNA dynamics. Probing of rapid dynamics requires sufficient fluorescence intensity to provide adequate signal-to-noise over a wide range of concentrations. The results in Figure 7A demonstrate that reactions on a 50-ms time scale can be studied with labeled oligomer at a concentration of 1.2 μM, after mixing. Stopped-flow studies of binding to ribozyme have been reported at a concentration as low as 50 nM.[28] Probing slow dynamics requires stability against photodegradation to allow data to be collected for long times. The results in Figure 7B indicate 5′-pyrene oligomers are stable for more than 25 min.

The properties of high fluorescence intensity with negligible photodegradation also make 5′-pyrene oligomers ideal for equilibrium measurements of binding constants for RNA oligomers. Current methods for such measurements include equilibrium dialysis,[53] gel retardation,[54,60–62] and filter binding.[63] Equilibrium dialysis measurements, however, require up to 3 days, while gel retardation and filter binding are not true equilibrium methods. A fluorescence titration with a 5′-pyrene oligomer required only 15 min for each point and a total time of about 1–2 h. For binding to the L-21 Sca I ribozyme, sufficient signal-to-noise is available down to 5 nM bound complex, allowing measurement of equilibrium constants as low as 5 nM.[28] For some systems, fluorescence melting experiments could be useful in providing enthalpic and entropic data in addition to binding constants.

The large increase in fluorescence observed upon binding of RNA substrates with pyrene attached to their 5′-end suggests such probes may be useful in a large number of applications. For example, they may be useful in probing the environment, length, and dynamics of RNA binding sites on RNAs and proteins, for localizing RNA processing machinery *in vivo*, and for studying RNA folding. Energy-transfer experiments should also be feasible and informative in many applications, including ribozyme kinetics. Since the pyrene fluorophore lacks functional groups, it may be possible to develop a pyrene phosphoramidite for direct coupling to the end of an oligomer chain.[24] Facile ligation of modified oligomers to large RNAs has been recently described.[64] This method would allow coupling of a 5′-pyrene oligomer to the 5′-end of any large RNA, which could provide a probe of intramolecular conformational changes. Nucleic acid hybridization experiments with fluorescence detection could be possible with a single label rather than double labels.[65,66]

**Acknowledgment.** We thank Professor Kenneth A. Johnson (The Pennsylvania State University) for use of his stopped-flow apparatus and for stimulating discussions, Jeffrey McDowell for assistance with energy minimization and molecular dynamics calculations, Jin-Feng Wang for helpful suggestions, and the Midwest Center for Mass Spectrometry at the University of Nebraska, Lincoln for performing mass spectra (funded by the National Science Foundation, Biology Division Grant DIR9017262). This research was supported by NIH Grant GM 22939 and the Office of Naval Research. P.C.B. is a Messersmith Fellow, and D.H.T. is a Guggenheim Fellow.

(59) Sugimoto, N.; Sasaki, M.; Kierzek, R.; Turner, D. H. *Chem. Lett.* **1989**, 2223–2226.

(60) Pyle, A. M.; McSwiggen, J. A.; Cech, T. R. *Proc. Natl. Acad. Sci. U.S.A.* **1990**, *87*, 8187–8191.

(61) Garner, M. M.; Revzin, A. *Nucleic Acids Res.* **1981**, *9*, 3047–3060.

(62) Fried, M.; Crothers, D. M. *Nucleic Acids Res.* **1981**, *9*, 6505–6525.

(63) Draper, D. E.; Deckman, I. C.; Vartikar, J. V. *Methods Enzymol.* **1988**, *164*, 203–220.

(64) Moore, M. J.; Sharp, P. A. *Science* **1992**, *256*, 992–997.

(65) Cardullo, R. A.; Agrawal, S.; Flores, C.; Zamecnik, P. C.; Wolf, D. E. *Proc. Natl. Acad. Sci. U.S.A.* **1988**, *85*, 8790–8794.

(66) Morrison, L. E.; Halder, T. C.; Stols, L. M. *Anal. Biochem.* **1989**, *183*, 231–244.

(67) Barshop, B. A.; Wrenn, R. F.; Frieden, C. *Anal. Biochem.* **1983**, *130*, 134–145.

(68) Zimmerle, C. T.; Frieden, C. *Biochem. J.* **1989**, *258*, 381–387.